

# Neutron flux measurements correlated to the Regener-Pfotzer Maximum.

Kaitlyn Blair<sup>a</sup>, Zoe Sternberg<sup>a</sup>, Hope Holte<sup>a</sup>, Anisa Tapper<sup>a</sup>, Erick Agrimson<sup>b</sup>

## Abstract

During the summer of 2022, St. Catherine's all-women's team expanded upon work with personal neutron dosimeters (PNDs) utilizing 1200 g helium-filled high-altitude balloons (HABs). The PND devices flown on the missions can detect the interaction with a neutron colliding with the tube material. The neutron collision creates a bubble that can be accompanied by a popping sound during this collisional event which is recorded via a digital camera. Neutrons measured via the PND are plotted in conjunction with the charged particle maximum known as the Regener-Pfotzer (R-P) maximum. The R-P maximum is a region created when a cosmic ray (often a proton) collides with atmospheric nuclei creating a shower of charged and neutral particles in the atmosphere resulting from the collision. Current work shows that neutron events have a peak flux in the 15,000 – 25,000 m range, which correlates with the charged particle R-P maximum altitude region. This means that both the charged and the neutral particles have a maximum number of detections in the same altitude region. In addition to improvements in video capture (i.e., lighting and glare reduction), the PND data have been expanded to include two tubes in each payload box paired with an omnidirectional Geiger-Müller tube. The experimental setup can now look at coincidences between the two PNDs, and the updated configuration adds to the statistics of neutron events on a given flight. The changes to the payload configurations within the box will be developed for research related to cosmic ray shower events occurring during the upcoming 2024 total solar eclipse.

Neutron Dosimeter 1 | Regener-Pfotzer Maximum 2 | Galactic Cosmic Rays 3 | ...

---

## 1. Introduction

Galactic cosmic rays have been of interest to the atmospheric ballooning community for well over a century. Studies of cosmic radiation began with the work of Victor Hess in a series of ballooning flights that took place between the years 1911 and 1913. The altitudes reached during the Nobel prize-winning experiments were up to 5km<sup>1</sup>. This research was followed up by the first stratospheric manned balloon by Piccard and Cosyns in 1933, reaching an altitude of 16km inside a pressurized capsule<sup>2</sup>. Peters<sup>3</sup> provides an extensive overview of the development of cosmic ray research from the mid-1940s up through the mid-1950s, including early high-altitude balloon (HAB) flights investigating cosmic rays. Grieder<sup>4</sup> has written a significant overview of cosmic ray research from the ground up to satellite measurements containing data collected up to the turn of the 21st century.

<sup>a</sup> Undergraduate student, St. Catherine University, 2004 Randolph Ave., St. Paul, MN, 55105.

<sup>b</sup> Associate Professor of Physics, St. Catherine University, 2004 Randolph Ave., St. Paul, MN, 55105,  
Author to whom correspondence should be addressed: Erick Agrimson, [epagrimson@stkate.edu](mailto:epagrimson@stkate.edu)

### 1.1 Mechanism of cosmic ray production

Galactic Cosmic Rays are constantly impinging Earth’s atmosphere, typically in the form of protons. These protons interact with atmospheric nuclei, and the resulting collision creates a cascade of high-energy secondary particles called a Galactic Cosmic Ray Shower (GCRS). Details of GCRSs depend on the altitude, latitude, and solar activity (following the 11-year solar cycle for lower energies) present on Earth<sup>4</sup>. GCRSs result from distant sources, such as stars or remnants of a supernova. By the time these secondary particles reach the Earth’s surface, they are primarily muons. Measurements must be made in situ to detect the most-diverse range of particles. GCRs, as described in ref. [4] and illustrated in Figure 2, can be classified into three main components: the electromagnetic (mostly photon-electron components) driven by neutral pion decay, the hadronic component (which constitutes the core portion of the showers), and the mesonic component driven mainly by the decay of pions into muons.

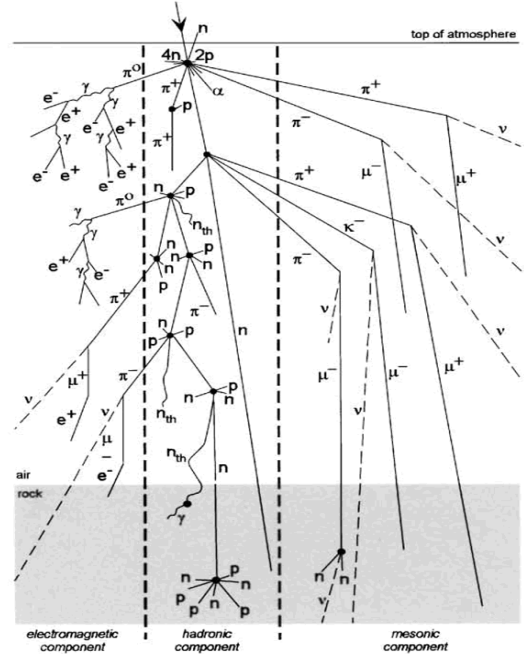


Figure 1: Components of a cosmic ray shower <sup>5</sup>.

### 1.2 The Regener-Pfotzer Maximum

Between 15,000 and 25,000 m altitude lies the Regener-Pfotzer (R-P) Maximum<sup>6-7</sup>. The charged particle maximum is the altitude at which the largest number of counts per unit time is measured with a Geiger-Müller (G-M) detector (also called a Geiger counter). The unit of measure used in data collection is counts per unit of time, where each count is the detection of a single high-energy particle or cascade. Depending on factors such as altitude, solar activity, pressure, temperature, density, and geomagnetic latitude, the R-P Maxima can occur at different altitudes<sup>8-10</sup>. In addition to the charged particles observed in the R-P maximum, the presence of neutrons is a part of the hadronic component of the GCRS and is the additional focus of the current work.

### 1.3 Neutral particle detection using Personal Neutron Dosimeters (PND's)

PND's<sup>11</sup> have the ability to detect the interaction due to a neutron collision with the material present inside of the PND. The process of the detection process is given in figure 2.

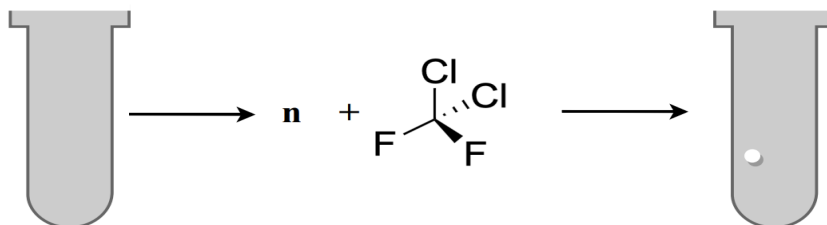


Figure 2: Diagram of PND neutron reaction. The white circle represents a bubble formed after a neutron ( $n$ ) has collided with the dosimeter material<sup>11</sup>.

## 2. Collection of Cosmic Ray Data

The neutron box, as we refer to this particular payload, consisted of one RM-60 (Radiation monitor) Geiger counter set to collect omnidirectional charged particle interactions via an Arduino Microcontroller with GPS saving data on a SD card. The charged particle data was averaged every one minute to determine the R-P maximum. A heater circuit is used to keep the inside box temperature at a reasonable level during the entirety of the flight. In addition, a camera (Go Pro® HERO 3 version) was used to observe a PND dosimeter manufactured by BubbleTech Industries®. In the most recent summer of 2022, the payload was flown with multiple PND's as to increase the statistics of a particular flight and to allow for coincidence (measuring neutron detections within fraction of a second of each other) which could be the same neutron interacting with both tubes. Other modifications made the summer of 2022 include the use of a LED light as opposed to a standard light bulb which had been flown in 2019 and 2021. (Future payloads will investigate the use of a LED light bar to see what effects that has on light refraction on the tube and optimization of detection of the neutron bubbles). The other significant development this summer was the use of grid line paper as to assist in the localization of neutron bubble formation within the tube. Figure 3 shows the setup of the neutron box as well as figure 4 the grid setup for summer of 2022. Figure 5 shows the whiteboard analysis of gridded data for the flight of 6-8-22.

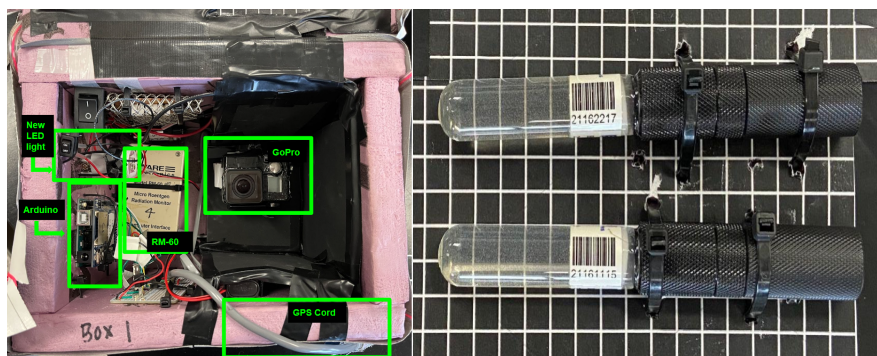


Figure 3 (left) The critical components of the neutron box.  
Figure 4 (right) PND's with grid paper.

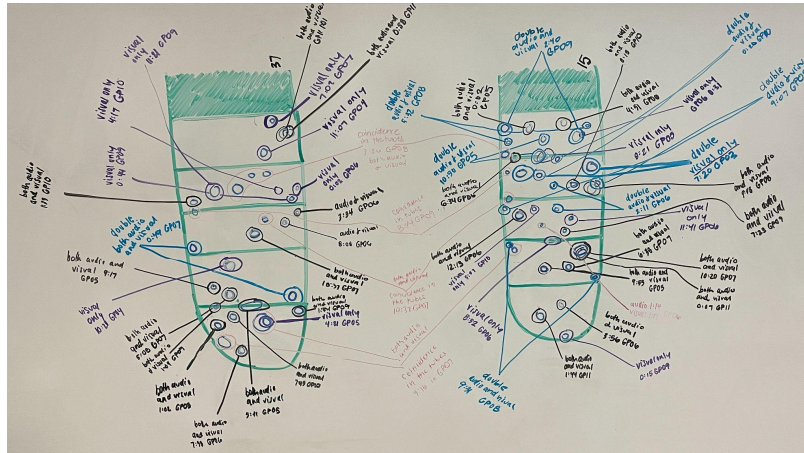


Figure 5. Bubble mapping from GoPro video of neutron tube to document altitudes at which bubbles form.

### 3. Results and Summary

A total of seven flights thus far have been flown with at least one PND and the RM-60 G-M omnidirectional detector, which measures the charged particles from the cosmic ray shower. The flight dates were as follows 6/7/19, 6/13,19, 7/27,19, 6/28,21, 7/8/21, 5/1,22 and 6/8/22. The last two flights carried multiple PNDs though data could only be extracted for one of the two tubes for the 5/1/22 flight. The 6/8/22 flight had two sets of PNDs, tubes 37 and 15 paired together and tube 17 with 28. (The numbering of the tubes came from the scan code provided by BubbleTech® Industries and provides a simple way to document and keep track of the tube when placed in view of the GoPro® camera).

#### 3.1 Documenting the number of bubbles.

Figure 6 is a QR code that links to video about the flight on 6/8/22 and the documentation of single, double and coincidence bubble formation that took place on this particular flight.



Figure 6. Video supplemental link showing formation of bubbles on the flight of 6/8/22.

### 3.2 Results from flight 6/8/22.

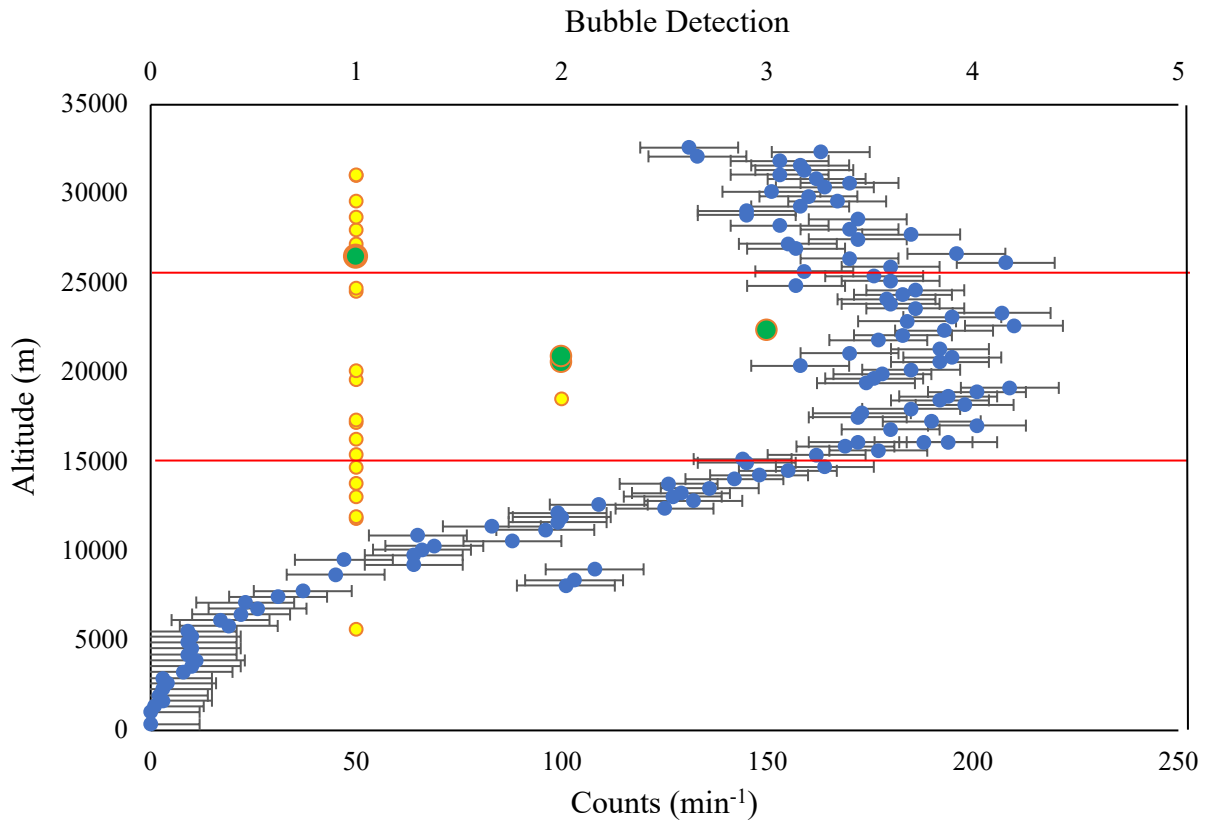


Figure 7. Data from tube 37 from the flight on 6/8/22. The blue circles are the one-minute averages of charged particle counts as detected by the RM 60 G-M detector. The yellow circles are the neutrons detected via the PND tube with noting of single, double and triple detections noted (i.e. a triple detection is where three bubbles show up at the same instant in time). The green circles are times when bubbles in tube 37 correspond with coincident bubble(s) in tube 15. The red lines are indicative of the charge particle R-P maximum<sup>6-7</sup>.

The data from tube 37 show a typical R-P maximum with a peak charged particle count of around 21,000 m, well within the published range<sup>6-7</sup>. Within this data set are six neutron detections below the R-P maximum, 12 within the range, and six above the range. Also of note is that four green circles appear, which indicates that four coincident bubbles were formed in the adjacent tube (tube 15). Of interest, three of these four events were not just single events in tube 37 but rather double events or triple events. The interpretation of this data could be many. It is possible that multiple neutrons interacted at the same instant in time. It is also possible that an energetic neutron was able to interact with both tubes during the small time frame. Yet another possibility is that a shower that involved multiple neutrons was created in the vicinity of the tubes. More flights, as well as additional feedback, are warranted to explain the possible mechanism more clearly.

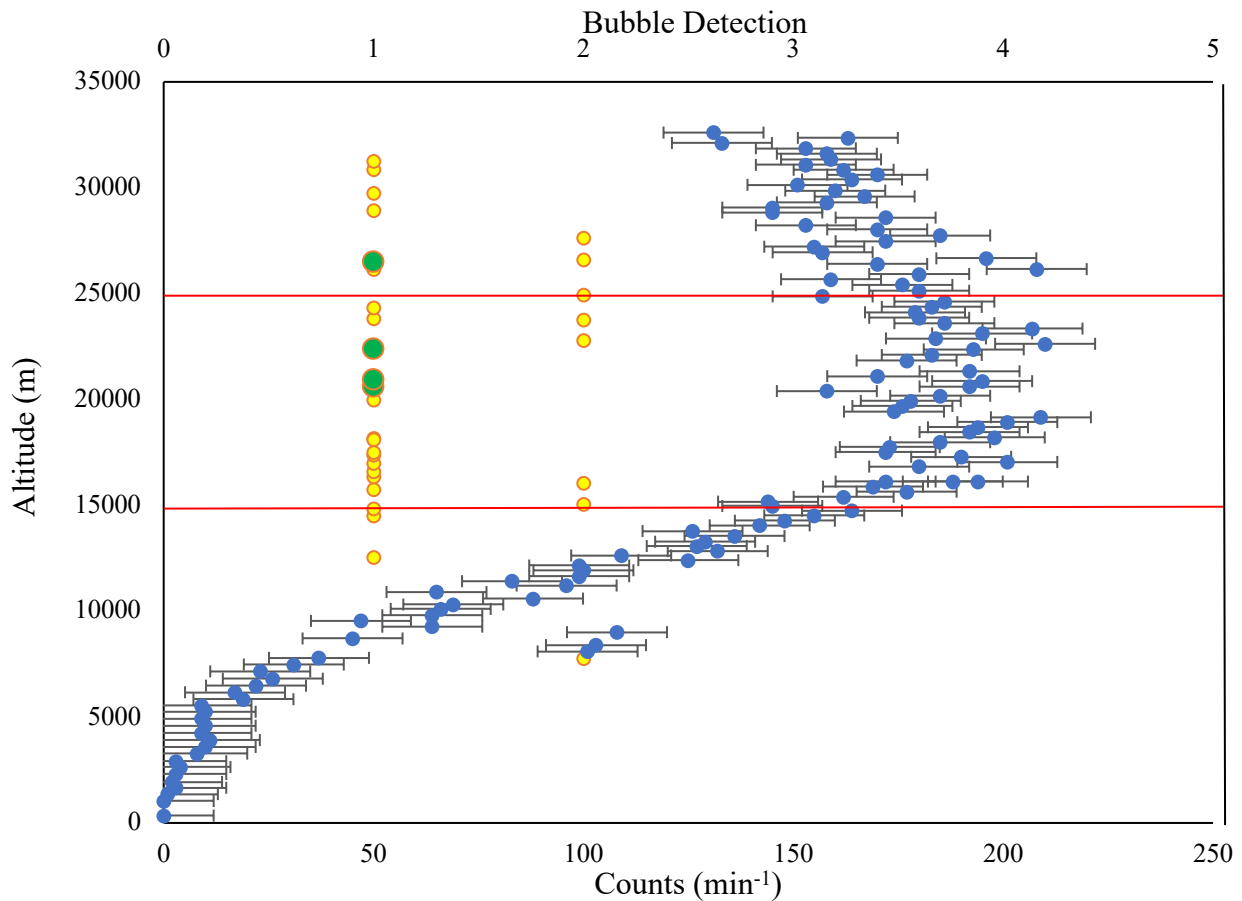


Figure 8. Data from tube 15 from the flight on 6/8/22. The blue circles are the one-minute averages of charged particle counts as detected by the RM 60 G-M detector. The yellow circles are the neutrons detected via the PND tube with noting of single, double and triple detections noted (i.e. a triple detection is where three bubbles show up at the same instant in time). The green circles are times when bubbles in tube 15 correspond with coincident bubble(s) in tube 37. The red lines are indicative of the charge particle R-P maximum<sup>6-7</sup>.

The data from tube 15 show a typical R-P maximum with a peak charged particle count of around 21,000 m, well within the published range 6-7. Within this data set are two neutron detections below the R-P maximum, 17 within the range, and nine above the range. Also of note is that four green circles appear, which indicates that four coincident bubbles were formed in the adjacent tube (tube 37). Of interest, all the events were just single events in tube 15. This is much different than what we observed in tube 37 – as to why this tube observed only single events. In contrast, the other tube did not observe any conjecture at best but does warrant the future work of more flights to see if the trend continues or is just an artifact of this particular flight.

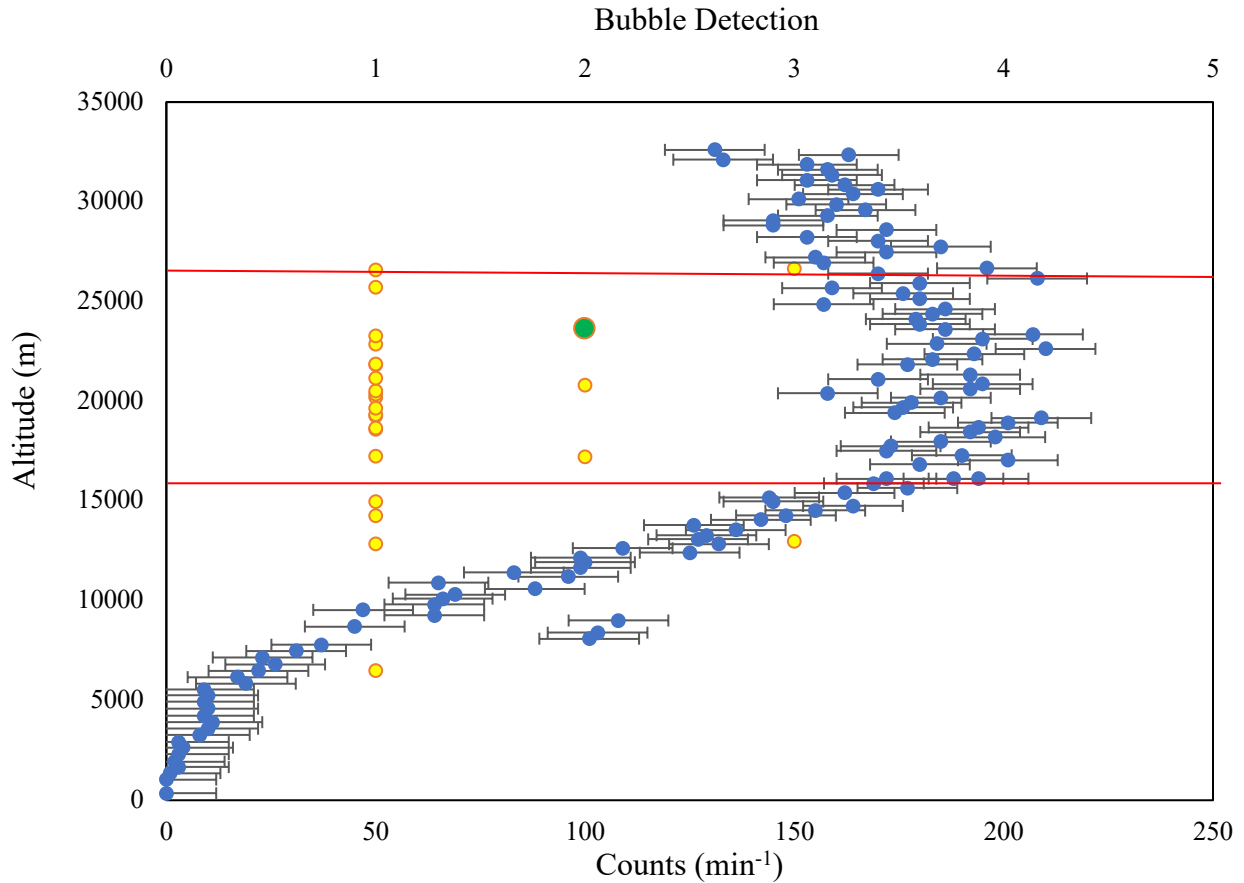


Figure 8. Data from tube 17 from the flight on 6/8/22. The blue circles are the one-minute averages of charged particle counts as detected by the RM 60 G-M detector. The yellow circles are the neutrons detected via the PND tube with noting of single, double and triple detections noted (i.e. a triple detection is where three bubbles show up at the same instant in time). The green circles are times when bubbles in tube 17 correspond with coincident bubble(s) in tube 28. The red lines are indicative of the charge particle R-P maximum<sup>6-7</sup>.

The data from tube 17 show a typical R-P maximum with a peak charged particle count of around 21,000 m, well within the published range 6-7. Within this data set are five neutron detections below the R-P maximum, 14 within the range, and one above the range. Also of note is that one green circle appears, which indicates that one coincident bubble was formed in the adjacent tube (tube 28). Of interest is a two-bubble formation in this tube, whereas a single bubble was formed in tube 28. Why this set of two tubes did not produce more events than the other payload will have to be an ongoing investigation.

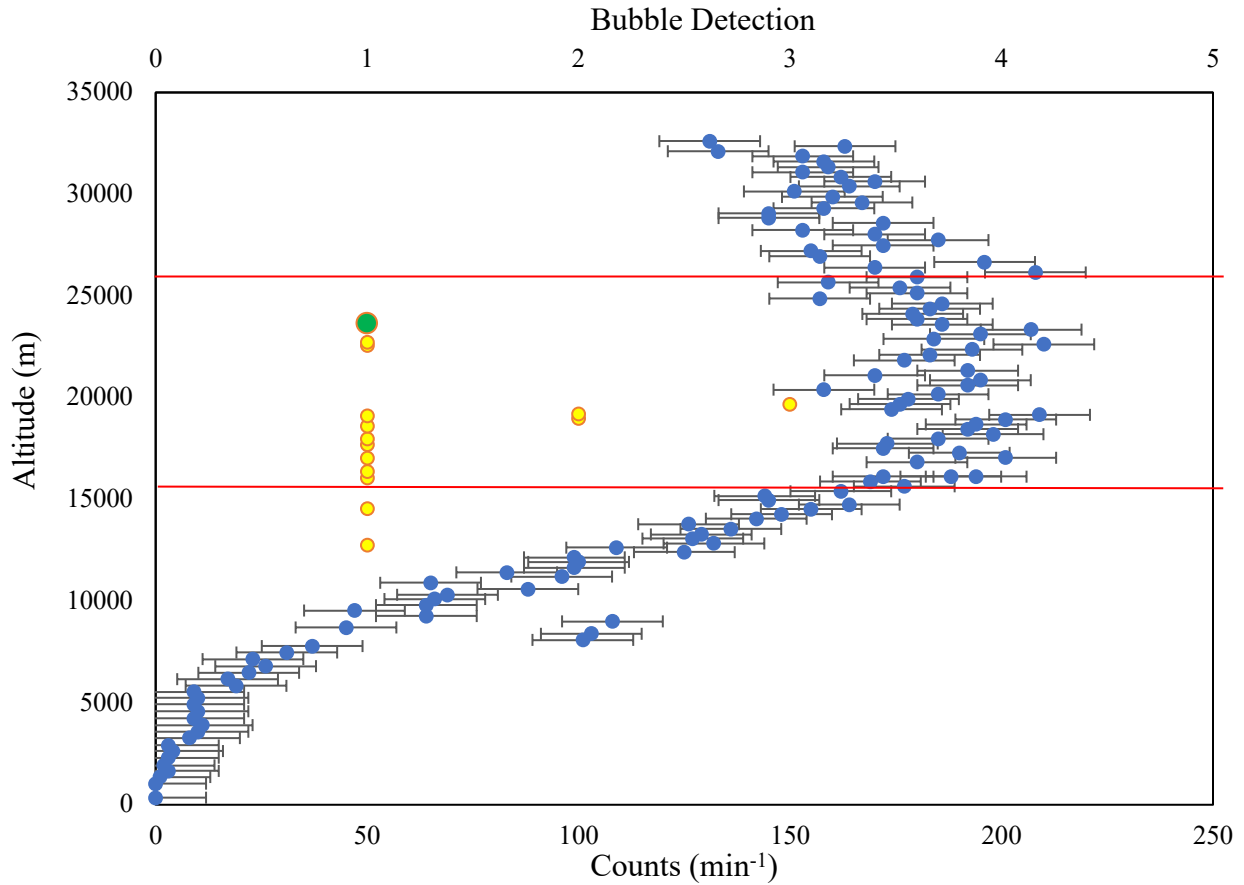


Figure 8. Data from tube 28 from the flight on 6/8/22. The blue circles are the one-minute averages of charged particle counts as detected by the RM 60 G-M detector. The yellow circles are the neutrons detected via the PND tube with noting of single, double and triple detections noted (i.e. a triple detection is where three bubbles show up at the same instant in time). The green circles are times when bubbles in tube 28 correspond with coincident bubble(s) in tube 17. The red lines are indicative of the charge particle R-P maximum<sup>6-7</sup>.

The data from tube 28 show a typical R-P maximum with a peak charged particle count of around 21,000 m, well within the published range 6-7. Within this data set are two neutron detections below the R-P maximum, 13 within the range, and, interestingly enough, no detections above the R-P maximum. The detection of no neutrons above the R-P maximum (short of having a height-limited flight) is unique to this particular tube on this particular flight. Results such as this one is why more flights are needed with this particular configuration to improve the overall statistical analysis. Also of note is that one green circle appears, which indicates that one coincident bubble was formed in the adjacent tube (tube 17).



### 3.3 Statistics for flight 6/8/22.

Table 1: Relative formation of bubbles for the 6/8/22 flight. The R-P maximum region is noted in red text.

Height range	Below 15,000 m	15,000 -25,000 m	Above 25,000 m
Bubble Percentage	17%	64%	19%

For the flight with the four PNDs flown, a significant number of neutron detections occur within the stated charged particle maximum known as the Regener-Pfotzer maximum. From this flight, it is clear that neutrons are also being produced in a significantly larger proportion than the regions outside the maximum region – the production region. Not only does it appear that the charged particles are reaching a maximum, but the neutral particles are also at a rate well outside of what is being obtained, either below 15,000 m or above 25,000 m. In addition, no bubbles were detected below 4,000 m, and in-ground tests, no bubble production has been observed for time frames up to one hour – which is also significant.

### 3.4 Overall statistics from flights 2019-2022 – the series of seven flights over a three-year span.

Table 2 shows the relative occurrence of the neuron bubble detections for all flights conducted in the PND study and gives an overview of the likelihood of a particular type of interaction.

Table 2: Relative formation for the PND flights. A double bubble for example is a formation of two bubbles at the same time in an individual tube.

Single Total Percentage	65.93%
Double Total Percentage	23.70 %
Triple Total Percentage	8.89 %
Quad Total Percentage	1.48 %

Over the entirety of all seven flights in the study thus far, the majority of the neutron detections have been of the single bubble variety. Interestingly enough a significant number of double bubble events have been documented with almost 24% of all events being double bubble detections.

Table 3: Altitude specific relative formation from the total number of PND flights. A triple bubble for example is three bubbles formed in an individual tube at the same time. The R-P maximum region is highlighted in red text.

Bubble Percentage	Below 15,000 m	15,000 -25,000 m	Above 25,000 m
Single Bubbles	18.89	32.59	14.44
Double Bubbles	3.71	14.82	5.19
Triple Bubbles	3.33	4.44	1.11
Quadruple Bubbles	1.48	0.00	0.00
Overall Percentages	27.41	51.85	20.74

Table 3 can be compared to the study of a single flight conducted in 2022. Of interest is that the number of events in the more extensive study show fewer neutron occurrences within the R-P max region and more occurring below the R-P maximum. Events above 25,000 do not differ much from the single flight and the larger data set. Additional flights will need to continue to be added to the data set to increase the significance of the set. Even still, it is clear from this table that most neutron

events are indeed occurring in the maximum charge particle region – again showing that the 15,000 to 25,000 m region is essential in understanding the cosmic ray shower mechanism region.

### 3.5 Flux and Fluence calculations.

Since the size of the PND in the neutron payload box is known, we were able to make an approximation for the neutron radiation delivered to the PND. Since the PND is calibrated for neutron dosage measurements we can quantify the exposure that the payload PND was exposed to. This measurement is of interest for biological payloads to quantify neutron exposure during a HAB flight. For the best approximation of the PND, we assumed geometry of a right circular cylindrical shape - see equation (1):

$$Area = 2\pi rh + 2\pi r^2 \quad (1)$$

The parameters for the PND are as follows: the diameter is given by manufacturer as 1.9cm and the radius is 0.95 cm. In addition, the length of detection area equals 4.5cm – this will be the h. The result given an approximate area of 32.53cm<sup>2</sup>.

Fluence is used in medical physics and radiation therapy to quantify the dose. In this case we are using the area of the chamber rather than the standard sphere of cross-sectional area. The fluence is then calculated using equation (2).

$$\varphi = \frac{\text{number}}{\text{Area}} \text{ with units of cm}^{-2} \quad (2)$$

We can also find the Flux which is the fluence change with respect to time which can be calculated using equation (3).

$$\dot{\varphi} = \frac{\text{number}}{\text{Area s}} \text{ with units of cm}^{-2} \text{ s}^{-1} \quad (3)$$

Using the average of the four tubes flown in 6/8/22 the flux values for pre-R-P max, R-P maximum and post R-P maximum regions were calculated and are indicated in table 3.

Table 3: Average flux rates from the four PND tubes flown on 6/8/22.

Altitude	Below 15,000 m	15,000-25,000 m	Above 25,000 m
Flux in (Neutrons/ cm <sup>2</sup> s)	5.025 x 10 <sup>-5</sup>	2.4375 x 10 <sup>-4</sup>	1.3075 X 10 <sup>-4</sup>

An analysis of this flux values show the following: The R-P Max (15-25 km) has a flux which is at 4.85 times the (0-15 km) rate. Also, the post R-P max (25-32 km) has flux which is at 2.60 times the (0-15 km) rate. Finally, the R-P Max (15-25 km) has a flux which is 1.86 times the post R-P region (25-32 km) rate.

## 4. Future Work

Our team is interested in exploring the use of multiple PNDs and payloads. The coincidences of bubbles across multiple tubes and payloads in the same stack will be investigated in the context of neutron trajectory. Possible implications of reusing PNDs for different flights affecting bubble counts are also discussed. Establishing protocols for detecting bubble formation with audio only in data is necessary for consistency going forward. Varying weather (i.e., temperature, humidity, precipitation, cloud cover) may affect bubble occurrences. Improvements on GoPro® placement in neutron payload will increase the effectiveness of data collection. This study and future studies are in preparation for the annular solar eclipse in 2023 and the total solar eclipse in 2024.

## Acknowledgments

NASA's Minnesota Space Grant Consortium: <https://www.mnspacegrant.org>

St. Catherine University APDC funding

St. Catherine University past HAB team members: Alynie Walter, Melissa Graham, Alisha Wiedmeier, Claire Weinzierl, Judy Panmany, Maddie Ross, Margaret Medini

University of Minnesota Morris Faculty and Alumna: Gordon McIntosh, Alaina Swanson

Minnesota Space Grant Associate Director: James Flaten

## References

- 1 Hess, V. F. The Nobel Prize in Physics 1936.  
URL: <https://www.nobelprize.org/prizes/physics/1936/hess/biographical/> [Retrieved March 30, 2018]
- 2 Piccard, A. and Cosyns, M. *Comptes rendus de l'academie de mathem*, 195 No. 1, 1932, p 604.
- 3 Peters, B. "Progress in Cosmic Ray Research since 1947" *Journal of Geophys. Research* 64, No. 2 1959.  
doi: 10.1029/JZ064i002p00155
- 4 Grieder, P. *Cosmic Rays at Earth* 2001.
- 5 URL: <https://malagabay.wordpress.com/2014/07/27/atmospheric-science-burying-beals-barometer/>  
[Retrieved March 30, 2018]
- 6 Regener, E., "New Results in Cosmic Ray Measurements," *Nature*, Vol. 132, 1933, pp. 696-698.  
doi: 10.1038/132696a0
- 7 Carlson, P., & Watson, A. A. (2014, November 18). *Erich Regener and the maximum in ionisation of the atmosphere*. In *History of Geophysics and Space Science*. [Retrieved March 30, 2018]  
URL: <https://arxiv.org/ftp/arxiv/papers/1411/1411.6217.pdf>  
doi: 10.5194/hgss-5-175-2014
- 8 Bhattacharyya, A. et al., "Variations of  $\gamma$ -Ray and particle Fluxes at the Sea Level during the Total Solar Eclipse of 24 October, 1995," *Astrophys. Space Science*, Vol. 250, 1997, pp. 313-326.  
doi: 10.1023/A:100040822978
- 9 Harrison, R., Nicoll, K., & Aplin, K., "Vertical profile measurements of lower troposphere ionization," *Journal of Atmospheric and Solar-Terrestrial Physics*, Vol. 119, 2014, pp.203-210. 2014.  
doi: 10.1016/j.jastp.2014.08.006
- 10 Mishev, A. "Short- and Medium- Term Induced Ionization in the Earth Atmosphere by Galactic and Solar Cosmic Rays," *International Journal of Atmospheric Sciences*. 2013.  
doi: 10.1155/2013/184508
- 11 PND reference ----need to find...